From solitary to colonial with zooid miniaturization: ancestral-state reconstruction based on NGS data of stolidobranch ascidians

Naohiro Hasegawa[1], Hiroshi Kajihara[2]

[1]*Department of Natural History Sciences, Graduate School of Science, Hokkaido University, Kita 10 Nishi 8 Kitaku, Sapporo, Hokkaido, 060-0810, Japan*

Email: hoya.hasegawa.ronbun@gmail.com

[2]*Faculty of Science, Hokkaido University, Kita 10 Nishi 8 Kitaku, Sapporo, Hokkaido, 060-0810, Japan*

Corresponding author: Naohiro Hasegawa (hoya.hasegawa.ronbun@gmail.com)

Keywords: bioinformatics, evolution, phylogenomics, RNA-seq, sessile animals, Tunicata

Abstract

The size of organisms has consistently intrigued researchers across various disciplines in biology. However, the evolutionary process of zooid miniaturization in colonial animals remained an enigmatic topic. The family Styelidae, within the ascidian order Stolidobranchia, showcases a diverse spectrum of coloniality, positioning it as an ideal candidate for delving into the intricacies of colonial evolution. In this research, we inferred a phylogenomic relationship mainly within Styelidae using transcriptomes of a total of 42 ascidians; from 17 species sampled in Israel and Japan and transcriptome data from 25 species sourced from a previous study and a database. Through ancestral-state reconstruction, our analysis indicated a clear directional change: following the acquisition of coloniality, zooids tended to become progressively smaller. This miniaturization is likely an adaptive response, enabling organisms to swiftly colonize limited marine substrate. We formulated a mathematical model suggesting that zooid miniaturization, due to living space constraints, would result in a faster asexual cycle and accelerated expansion in a colony. Our data also suggested that coloniality evolved independently three times within Styelidae. Moreover, once colonial traits are established, they appear to be consistently preserved, underscoring their biological importance in the colonial lineage.

Introduction

The body size of organisms has been a matter of research topic among biologists, with its related factors so far considered including latitudinal variations, physiological implications, and life history strategies (Grischenko et al. 2002). Yet, much of our understanding of the evolutionary shifts in animal body size is derived primarily from solitary metazoans rather than colonial ones (Liow and Taylor 2019).

Colonies of sessile aquatic animals consist of modular individuals, termed polyps and zooids (Beklemishev 1969). The modules within a single colony are clones, proliferating through asexual reproduction (Ryland and Warner 1986). Coloniality has independently evolved across various animal higher taxa (Hiebert et al. 2021), including Bryozoa (Schwaha et al. 2020), Cnidaria (Barbeitos et al. 2010; Kayal et al. 2018), Hemichordata (Cannon et al. 2013), Kamptozoa (Fuchs et al. 2010), and Tunicata (Alié et al. 2021). Within each taxon, the modules of colonial organisms are typically smaller than solitary individuals (Ryland and Warner 1986; Mukai 2001). Although zooid miniaturization has been noticed in various taxa for approximately 40 years (e.g., Kott 1985; Ryland and Warner 1986; Davidson et al. 2004; Sogot et al. 2014; Kocot 2016; Braun and Stach 2018; Nanglu et al. 2023), its evolutionary process still remains a topic

of inquiry.

Ascidians, commonly known as sea squirts, exhibit a wide range of life history strategies (Satoh 1994; Burighel and Cloney 1997; Davidson et al. 2004). Within Ascidiacea, the order Stolidobranchia has been recognized as an ideal group for exploring the evolutionary plasticity of coloniality (Zeng et al. 2006; Pérez-Portela et al. 2009; Brown and Swalla 2012; Alié et al 2021). This order encompasses three families, Molgulidae, Pyuridae, and Styelidae (cf. Kott 1985; Monniot et al. 1991). While both molgulid and pyurid ascidians are solitary, styelids comprise solitary and colonial species (cf. Kott 1985; Monniot et al. 1991). Kott (1985) classified Styelidae into three subfamilies: Botryllinae, which includes colonial forms with systems—zooids' arrangements around common cloacal cavities in a colony; Polyzoinae, which comprises colonial forms without systems; and Styelinae, which consists solely of solitary forms.

Among the colonial groups, a diverse range of coloniality has been observed (Fig. 1). In terms of the degree of colonial complexity, the polyzoine genus *Symplegma* Herdman, 1886 positions between other polyzoines and the highly integrated botryllines (Shirae et al. 1999; Gutierrez and Brown 2017). There is no morphological difference between the colonial genus *Syncarpa* Redikorzev, 1913 and the solitary genus

71 *Dendrodoa* MacLeay, 1824 except forming colonies (Hasegawa and Kajihara 2019).
72 The diversity of coloniality in Styelidae is actualized by various budding modes, which
73 can be categorized based on the tissues from which buds (= daughter zooids) originate
74 in mother zooids. Specifically, three budding modes are recognized: basal budding (Alié
75 et al. 2018), peribranchial budding (Metschnikoff 1869; Pizon 1893; Ritter 1896; Selys-
76 Longchamps 1917; Berrill 1940, 1948; Watanabe and Tokioka 1972; Mukai and
77 Watanabe 1976; Kawamura and Watanabe 1981; Akhmadieva et al. 2007), and vascular
78 budding (Giard 1872; Oka and Watanabe 1957; Sabbadin et al. 1975; Nakauchi 1982;
79 Brunetti and Mastrototaro 2004; Brown et al. 2009; Kawamura and Sunanaga 2010;
80 Gutierrez and Brown 2017).
81 Phylogenetic analyses of Stolidobranchia based on partial sequences of 18S
82 rRNA and mitochondrial cytochrome *c* oxidase subunit I genes have variably suggested
83 that coloniality evolved once (Zeng et al. 2006; Tsagkogeorga et al. 2009; Hasegawa
84 and Kajihara 2019) or seven times (Pérez-Portela et al. 2009), but these studies often
85 yielded trees with less-supported nodes. Alié et al. (2018) suggested that peribranchial
86 budding and basal budding evolved convergently, and that vascular budding was
87 secondarily derived in an ancestor exhibiting peribranchial budding, based on a
88 phylogenomic tree with high support values. However, their analysis (Alié et al. 2018)

lacked some key taxa, such as *Symplegma* and *Syncarpa*, which are pivotal for discussions on the evolution of coloniality. While the phylogenetic relationships in Stolidobranchia have been inferred by many previous authors to elucidate how coloniality evolved, no attempt has been made to reconstruct the ancestral states of coloniality using statistical methods.

The aim of this study is to clarify the evolutionary relationship between zooid size and coloniality. A robust phylogenomic tree was constructed, encompassing key taxa in the Stolidobranchia essential for understanding the evolution of coloniality. Through Bayesian inference for ancestral-state reconstruction, we provide a clear depiction of trait evolution related to coloniality on the tree. Additionally, we propose a mathematical model suggesting that zooid miniaturization has been driven by spatial competition on substrates.

Methods

Sampling, fixation, and identification. A total of 17 ascidian species, including both colonial and solitary forms, were sampled in Israel and Japan from May 2021 to January 2023 (Table 1). We conducted taxon sampling without bias in body size. The animals were anesthetized with menthol. For solitary individuals, oral or atrial siphons were

107 excised and preserved in RNAlater; the remaining bodies were preserved in 10%
108 formalin. For colonial forms, a part of the colonies was cut off and preserved in
109 RNAlater; another part was preserved in 10% formalin. The RNAlater-preserved
110 specimens were used for total RNA extraction; the formalin-fixed specimens were used
111 for morphological identification. For specimens collected in Israel, 1% borax was added
112 to the formalin fixative solution.

113 **RNA extraction, purification, and sequencing.** The tissues preserved in
114 RNAlater were homogenized in tubes containing 500 mL of Sepazol-RNA I Super G
115 (Nacalai tesque, Kyoto). The homogenate was left at room temperature for 5 minutes
116 and then mixed with 100 μL of chloroform. Then, the samples were centrifuged at
117 12,000 × g for 15 minutes. 250 μL of upper aqueous phase was mixed with 250 μL of
118 isopropanol and 0.5 μL of glycogen solution, followed by incubation at room
119 temperature for 10 minutes. Subsequently, they were centrifuged at 12,000 × g for 10
120 minutes. The solution was removed from tubes, and 500 μL of 80% ethanol was added.
121 After centrifugation at 12,000 × g for 5 minutes, the ethanol was carefully removed;
122 then, pellets were air-dried. The pellets were dissolved in 200 μL of TE to obtain crude
123 RNA extracts. The crude RNA solution (dissolved in 200 μL of TE) was added to 200
124 μL of a mixture of phenol:chloroform:isoamyl alcohol (25:24:1). The samples were

125 centrifuged at 13,000 rpm for 10 minutes at room temperature. Upper aqueous phase
126 was transferred to a new tube; then, 200 μL of chloroform:isoamyl alcohol (24:1) was
127 added. Once more, after centrifugation at 13,000 rpm for 10 minutes at room
128 temperature, 180 μL of upper aqueous phase was collected. To this, 20 μL of 3M
129 sodium acetate solution, 500 μL of 100% ethanol, and 0.5 μL of glycogen solution were
130 added. The samples were then centrifuged at 15,000 rpm for 30 minutes at 4°C, and the
131 supernatant was removed. Pellets were mixed with 700 μL of 80% ethanol, followed by
132 centrifugation at 15,000 rpm for 5 minutes at 4°C. The supernatant was removed, and
133 pellets were air-dried. The pellets were dissolved in 10 μL of TE to obtain total RNA
134 solutions. Concentration of total RNA in the solution was measured using a NanoDrop
135 (Thermo Fisher Scientific). The volume of the solution containing 5 μg of RNA was
136 measured; then, pure water was added to adjust the total volume to 26.5 μL; for samples
137 that did not meet the 5 μg threshold, the entire volume of the total RNA solution was
138 added. For removing DNA from the samples, 3 μL of 10 × TURBO DNase buffer
139 (Thermo Fisher Scientific) and 0.5 μL of TURBO DNase (Thermo Fisher Scientific)
140 were added. The samples were incubated at 37°C for 30 minutes using a 2720 thermal
141 cycler (Thermo Fisher Scientific). After incubation, 3 μL of DNase Inactivation Reagent
142 (Thermo Fisher Scientific) was added, and the samples were incubated at room

143 temperature for 5 minutes with tapping every 2 min. Subsequently, the samples were
144 centrifuged at 10,000 × g for 2 minutes at room temperature, and 25 μL of supernatant
145 was collected. To the supernatant, 75 μL of water, 10 μL of 3M sodium acetate solution,
146 0.5 μL of glycogen solution, and 275 μL of 100% ethanol were added. The samples
147 were centrifuged at 15,000 rpm for 30 minutes at 4°C; then, the supernatant was
148 removed. Pellets were mixed with 400 μL of 80% ethanol, followed by centrifugation at
149 15,000 rpm for 5 minutes at 4°C. Once more, supernatant was removed; the pellets were
150 air-dried. The pellets were dissolved in 11 μL of pure water to obtain total RNA
151 solutions free of genomic DNA. Concentration of RNA in the solutions was measured
152 using a NanoDrop (Thermo Fisher Scientific). Absence of RNA degradation was
153 confirmed by electrophoresis. cDNA library preparation and paired-end sequencing
154 were performed by Novogene; the Illumina NovaSeq 6000 was used for next-generation
155 sequencing.

156 **Phylogenomic analysis.** For obtaining *de novo* transcriptomes, we mainly
157 followed Alié et al. (2018). The following three types of Illumina reads were filtered by
158 Novogene: reads containing adapter contamination, with more than 10% of bases that
159 could not be determined throughout the entire length, and where more than 50% of
160 bases had Q20 of Phred value (Ewing et al. 1998) in their entire length. The reads data

161 was registered as the BioProject PRJNA880804 in Sequnce Read Archive (SRA). The
162 filtered reads were *de novo* assembled with Trinity ver. 2.8.5 (Grabherr et al. 2011)
163 using default parameters. Open reading frames (ORFs) with less than 90 amino acids
164 were discarded by TransDecoder ver. 5.5.0
165 (https://github.com/TransDecoder/TransDecoder; last accessed May 2023). ORFs
166 having similar nucleotide sequences were clustered using CD-HIT-EST ver. 4.8.1 (Li
167 and Godzik 2006; Fu et al. 2012) with default parameters. The reads were mapped on
168 the remaining contigs by using Kallisto ver. 0.46.2 (Bray et al. 2016). The contigs that
169 had low expression levels were picked up by drawing density plots with R; the contigs
170 were retained based on the threshold corresponding to the lower peak of the plot. To
171 assess the accuracy of the sequencing, BUSCO ver. 5.3.2 (Simão et al. 2015;
172 Waterhouse et al. 2017; Seppey et al. 2019; Manni et al. 2021) with metazoan datasets
173 was used to examine the presence of core gene sets in the assembled sequences. Cross-
174 contamination occurring in the process from the extraction to the RNA-seq was
175 removed using CroCo (Simion et al. 2018). In addition to the *de novo* transcriptomes,
176 16 transcriptomes were downloaded from a GitHub repository, styelidae (Alié et al.
177 2018; https://github.com/AlexAlie/styelidae) for a phylogenomic analysis (Table 2);
178 core proteomes of nine ascidian species were also downloaded from Ascidian Network

179 for In Situ Expression and Embryological Data (ANISEED) (Table 2). I retained only
180 the longest sequence for each gene in their respective proteomes from each of the nine
181 species; CD-HIT ver. 4.8.1 (Fu et al. 2012) was used for dereplicating with -c *1.0*
182 option, for excluding sequences consisting of less than 30 amino acids.

183 Multiple alignments were constructed for the phylogenomic analysis.
184 Orthologous clusters were built based on the proteomes from 42 species using
185 OrthoFinder ver. 2.5.4 (Emms and Kelly 2015) with -M *msa* and -S *blast* options. The
186 sequences were downsampled within each cluster that had multiple sequences derived
187 from the same sample; the longest sequence was designated as the representative
188 sequence for each species. From these downsampled clusters, we excluded the clusters
189 that did not meet the following criteria: within each cluster, *i*) containing 30 or more
190 sequences of the total 33 species listed in Table 1 and from the GitHub repository
191 styelidae (Table 2); and *ii*) containing seven or more sequences of the nine species from
192 ANISEED (Table 2). For these two steps, we utilized a Python script in the GitHub
193 repository Directionality_zooid_miniaturization
194 (https://github.com/231007NHasegawa/Directionality_zooid_miniaturization). Each
195 remained cluster was aligned by MAFFT ver. 7.520 (Katoh and Standley 2013) with *E-*
196 *INS-i* strategy. The alignments were individually trimmed using TrimAl ver. 1.4. rev. 15

197 (Capella-Gutiérrez et al. 2009) with *strictplus* method. Then, the trimmed alignments
198 were concatenated with each other by my original Python script
199 (https://github.com/231007NHasegawa/Directionality_zooid_miniaturization).
200 Maximum Likelihood (ML) analysis and Bayesian inference (BI) were
201 performed based on the concatenated alignment for inferring a phylogenetic relationship
202 among Stolidobranchia. Prior to conducting the ML analysis, the substitution models
203 corresponding to each partition in the multiple alignment were selected with
204 ModelFinder program (Kalyaanamoorthy et al. 2017) referring partition models
205 (Chernomor et al. 2016) implemented in IQ-TREE ver. 2.2.2.6 (Minh et al. 2020); then,
206 the ML analysis was conducted by IQ-TREE ver. 2.2.2.6 (Minh et al. 2020) with
207 ultrafast (UF) bootstrap method (Hoang et al. 2018). Branch support values were
208 evaluated with 1,000 UF bootstrap replicates. BI analysis was performed using the MPI
209 version of ExaBayes ver. 1.5.1 (Aberer et al. 2014). Two independent MCMC runs were
210 parallelly run, started from a random tree; cold chain and heated chain with 0.5 of
211 "heatFactor" option were executed per independent run. The runs were stopped that
212 each chain was run for 500,000 generations; at that time, the average standard deviation
213 of split frequencies reached 0.0%. Trees were sampled every 100 generations; the initial
214 25% of sampled trees were discarded as burn-in. Convergence was checked by

postProcParam program implemented in ExaBayes.

Ancestral-state reconstruction. To determine values for matrix entries in transition probability matrices for each character—*i*) basal budding, *ii*) peribranchial budding, *iii*) vascular budding, *iv*) common cloacal cavity, and *v*) coloniality (colonial or solitary)—we initially computed a maximum likelihood estimate by using "MultiState" (Pagel et al. 2004) as implemented in BayesTraits ver. 4.0.1 (http://www.evolution.reading.ac.uk/BayesTraitsV4.0.1/BayesTraitsV4.0.1.html; last accessed September 30th, 2023) for a transition rate of each character state. The rates calculated as zero were simply adjusted to 0.01 in the matrices, indicating that such transitions were rare evolutionary events. Subsequently, we conducted Bayesian inferences (BI) using "MultiState" (Pagel et al. 2004) based on the ML tree with 10,000,000 iterations, a burn-in of 2,500,000, a sampling frequency of 1,000, and the "ScaleTrees" option set at 0.1 because a mean of branch lengths of the ML tree was ca. 0.1. I employed a uniform distribution as a non-informative prior, adjusting an interval such that the transition probability matched the mean of the uniform distribution. Expected a posteriori (EAP) was computed to represent the posterior probabilities (PPs) of the character states at each node.

For the ancestral-state reconstruction, we obtained literature-based data of the

233 longest body length for each species based on taxonomic descriptions (Table 3). For
234 *Botrylloides* sp., *Microcosmus* sp., and *Styela* sp., the body lengths were measured
235 based on the formalin-fixed specimens. Information about the body length of *Polycarpa*
236 sp. is lacking (Alié et al. 2018). Based on the phylogenomic tree, MCMC analysis was
237 conducted selecting Brownian motion model by "Continuous: Random Walk" (Pagel
238 1999) with 10^8 iterations, 25% of burn-in, and the "ScaleTrees" option set 0.1. The body
239 length of each node was represented by a mean of values sampled from every 1,000
240 generations.

241 **Character correlation analysis.** To test the correlation between coloniality
242 and body length reconstructed on the tree nodes (whether or not there is any
243 evolutionary tendency between these characters), we utilized the "Test trait correlations:
244 continuous" and "Independent Contrast: Correlation" (Felsenstein 1973; Freckleton
245 2012) in BayesTraits version 4.0.1. Both MCMC approaches were adopted, employing a
246 stones command, setting 100 stones with 1,000 iterations each to determine a marginal
247 likelihood. Subsequent analyses were implemented using the "TestCorrel" command,
248 which sets the covariance to zero, employing identical command parameters as the first
249 analysis. Log Bayes Factor (Log BF) was calculated by taking twice the difference of
250 log marginal likelihoods between the two analyses.

251 **Detection of evolutionary direction.** The resulting tree included a subclade
252 solely consisting of members that undergo peribranchial budding (= Clade A, see
253 below). To evaluate if the body size evolved directionally in the entire Stolidobranchia
254 and this subclade, respectively, MCMC analyses were separately conducted based on
255 the whole of the ML tree and this subclade. First, an MCMC analysis was executed with
256 the command selecting "Continuous: Random Walk (Model A)" (Pagel 1999) and a
257 stones command estimating a marginal likelihood using 100 stones and 1000 iterations
258 per stone. Second, another MCMC analysis was carried out with the "Continuous:
259 Directional (Model B)" method (Pagel 1999), maintaining the same parameters for the
260 stones command. Then, the Log BF was computed by subtracting the log marginal
261 likelihood of the Model A and Model B. In addition, we calculated correlation
262 coefficient between body length and branch length for solitary and colonial forms.
263

264 **Results**

265 **Phylogenomics.** The number of Illumina reads after filtration obtained from 17 species
266 ranged from 42 million to 137 million. Through the assembly process, 26,116–108,633
267 contigs were kept for each species (Table 4). These contigs, along with transcriptomes
268 of 16 species from Alié et al. (2018) and proteomes of nine species from ANISEED,

269 were clustered in 360,094 orthologous groups. The number of orthologous groups that
270 met the filtration criteria were 1,883 out of 360,094. After alignment, trimming, and
271 concatenation, the dataset comprised 1,039,648 aa including gaps of 42 ascidian species
272 with 0.1% of missing data. The dataset was partitioned into 130 blocks; the best-fit
273 model was selected in each partition.

274 Almost all the nodes in the tree received highly supported values (100% UF
275 bootstrap; 1.00 PP); as an exception, the clade of *Eusynstyela tincta* + *E. latericius* + *E.*
276 *misakiensis* has 85% UF bootstrap value (Fig. 2). The order Stolidobranchia was sister
277 to the clade Aplousobranchia + Phlebobranchia. Phlebobranchia was non-monophyletic;
278 in it, *Phallusia* was sister to Aplousobranchia. In Aplousobranchia, *Aplidium* formed a
279 clade with *Pseudodistoma*. In Stolidobranchia, Molgulidae was inferred to have
280 branched off first from the rest of this group; Styelidae was recovered as monophyletic,
281 which turned out to be sister to a part of paraphyletic Pyuridae. In Styelidae, members
282 that perform peribranchial budding—botryllines and part of polyzoines—formed a clade
283 (hereafter Clade A); in Clade A, *Symplegma* was sister to Botryllinae (*Botrylloides* and
284 *Botryllus*). *Syncarpa* grouped together with paraphyletic *Dendrodoa*.

285 **Ancestral-state reconstruction.** The EAPs for the coloniality-related character
286 states—either *i*) budding from basal stolon, *ii*) budding from peribranchial epithelium,

287 *iii*) budding from blood vessel, *iv*) with a common cloacal cavity, or *v*) non colonial

288 (i.e., solitary)—exceeded 99% in every node (Figs 3–7).

289 **Character correlation.** The log marginal likelihoods were −240.18 and

290 −239.98 using complex models in "Test trait correlations: continuous" and

291 "Independent Contrast: Correlation", respectively, for testing whether there is a

292 correlation between the characteristic states of coloniality and body/zooid length; the

293 log marginal likelihoods with simple models setting the covariance to zero were

294 −242.32 and −242.26, respectively. The log BFs were 4.29 and 4.56, respectively; the

295 values exceeded two, which means positive evidence of correlation between the

296 character states in the two traits.

297 **Evolutionary direction.** The log marginal likelihood based on the entire

298 phylogenetic tree using Model A was −239.80. When using Model B, the value was

299 −240.47. From these two values, the Log BF was calculated to be 1.34. This value is

300 smaller than the threshold value of two, which does not support directionality in trait

301 changes. Based on Clade A, the value using Model A was −109.33; it was −112.35 using

302 Model B. The Log BF was 6.05; as it falls within 5–10, the presence of directionality

303 was strongly supported.

304 The correlation coefficients between body lengths and branch lengths were

305 0.01 for solitary forms and −0.85 and colonial forms, respectively. The slopes of the
306 regression lines for these two parameters were ca 2.8 in solitary form (coefficient of
307 determination: $R^2 = 0.0002$) and ca. −46.3 in colonial form ($R^2 = 0.7292$), respectively
308 (Fig. 8).
309
310 **Discussion**
311 This study indicates that zooids became gradually smaller once coloniality was acquired
312 (Figs 7, 8). To explain this evolutionary pattern, we hypothesize that zooid
313 miniaturization would shorten the period for daughter zooids to start budding (typically,
314 as an animal's body size increases, the time it requires to reach maturity also extends;
315 Blueweiss et al. 1978), leading to rapid expansion of the colony over substrates (Fig. 9).
316 The marine substrates represent a significant limiting resource for sessile organisms,
317 with living space being at a premium (Connell 1961; Pequegnat 1964; Dayton 1971;
318 Paine 1971; Jackson 1977, 1985; Hughes 2005; Tyrrell and Byers 2007). Colonial
319 invertebrates achieve this by continuously covering the substrate and exhibiting rapid
320 lateral growth through asexual reproduction with a rate of expansion, which is
321 unattainable through sexual reproduction alone (Jackson 1977).
322 The relationship between the substrate encrusting rate of a colony and the

zooid size at maturity can be mathematically described as follows. Let $A_C(t)$ be the colony area at time t, V_Z be the zooid volume at maturity, and k be the zooid's volume–growth rate per unit time. The growth rate of colony area per unit time can be expressed by the following equation:

$$\frac{dA_C}{dt} = \frac{k \cdot A_C}{V_Z} \tag{1}$$

because the area of a colony increases proportionally to the number of zooids in the colony, which is proportional to the colony area. Solving Eq. (1) yields:

$$\int \frac{dA_C}{A_C} = \int \frac{k}{V_Z} dt \tag{2}$$

$$ln|A_C| = \frac{kt}{V_Z} + C \tag{3}$$

where C is an integration constant. Since $A_C > 0$, Eq. (3) can be rearranged as:

$$A_C = e^{\left(\frac{kt}{V_Z} + C\right)} \tag{4}$$

where e indicates Euler's number. Setting $B = e^C$ (B is a constant), we yield

$$A_C = Be^{\frac{kt}{V_Z}}. \tag{5}$$

Plugging $t = 0$ in Eq. (5), we obtain:

$$A_C = B. \tag{6}$$

The initial value of the colony area $A_C(0)$ is equal to the area of a single zooid that arises when the larva attaches to the substrate and then metamorphoses. If we denote the zooid area as A_Z, the initial condition $A_C(0)$ equals to A_Z. Plugging this into Eq. (6), we obtain:

$$A_{\mathrm{C}}(t) = A_{\mathrm{Z}} e^{\frac{kt}{V_{\mathrm{Z}}}}. \tag{7}$$

By considering Eq. (7), the competition between two colonies with different zooid volumes and areas can be examined. Let us assume that Colony 1 possesses a larger zooid volume and area compared to Colony 2 (with $A_{\mathrm{Z1}} > A_{\mathrm{Z2}} > 0$ and $V_{\mathrm{Z1}} > V_{\mathrm{Z2}} > 0$), while their respective zooid's volume growth rates, denoted as k_1 and k_2 (each being a constant). Commencing at $t = 0$, both Colony 1 and Colony 2 originate from a single zooid, where the initial areas can be expressed as $A_{\mathrm{C1}}(0) = A_{\mathrm{Z1}}$ and $A_{\mathrm{C2}}(0) = A_{\mathrm{Z2}}$. The value of t at which the areas of both colonies become equivalent is determined by the following equation:

$$t = \frac{lnA_{\mathrm{Z2}} - lnA_{\mathrm{Z1}}}{\frac{k_1}{V_{\mathrm{Z1}}} - \frac{k_2}{V_{\mathrm{Z2}}}}. \tag{8}$$

In scenarios where k_2/V_{Z2} exceeds k_1/V_{Z1}, the implication is that Colony 2, with its smaller zooids, will eventually surpass the area of Colony 1, which comprises larger zooids (Fig. 25). Conversely, if k_2/V_{Z2} is less than k_1/V_{Z1}, the resultant negative value of t suggests that the area of A_{C2} will not overtake that of A_{C1}. Therefore, this model implies that Colony 1 must accelerate the growth rate of its zooids to achieve a faster colony expansion than Colony 2.

It is important to note here that the model merely discusses the advantages of smaller zooids in colony expansion rates and does not necessarily indicate that colonies

359 with smaller zooids will invariably produce more offspring in subsequent generations.
360 At least three disadvantages with smaller zooids can be conceived: *i*) the zooids would
361 become physically weaker, *ii*) they would be more susceptible to external environmental
362 impacts on the body surface, and *iii*) the number of eggs or sperm per zooid would be
363 reduced. The size of the zooids would be determined by a trade-off with these
364 disadvantages. Moreover, even when the two curves intersect as depicted in Eq. (8) and
365 Fig. 9, the lineage of Colony 1 does not necessarily go extinct if the colony succeeds to
366 form a sufficiently large area to reproduce for the next generation before the time of
367 intersection.

368 Coloniality was independently acquired at least three times in the evolutionary
369 history of Stolidobranchia (Fig. 7). These results contrast with previous phylogenetic
370 and phylogenomic analyses; acquisition of coloniality was inferred to occur only once
371 (Zeng et al. 2006; Tsagkogeorga et al. 2009; Hasegawa and Kajihara 2019) or at least
372 seven times independently (Pérez-Portela et al. 2009) based on 18S and COI, and at
373 least twice based on transcriptome data (Alié et al. 2018). In addition, the phylogenomic
374 tree, with high support values, supported the view that *Symplegma* would be an
375 intermediate group between other polyzoines and botryllines, an idea earlier proposed
376 based on morphological and immunological evidence (Shirae et al. 1999; Gutierrez and

377 Brown 2017). These results indicate that part of descendants from the last common
378 ancestor of the ascidians that undergo peribranchial budding sequentially acquired
379 vascular budding and common cloacal cavity. The result that the genus *Syncarpa* did not
380 form a clade with other colonial ascidians suggests the potential discovery of a new
381 budding mode or convergent evolution of peribranchial/basal budding in the future; the
382 budding mode has not been recorded in *Syncarpa* (cf. Redikorzev 1913; Tokioka 1951;
383 Sanamyan 2000; Hasegawa and Kajihara 2019).

384 In the evolution of coloniality within Stolidobranchia, once traits related to
385 coloniality were acquired, it seemed hard to lose them. The phylogenetic tree did not
386 depict evolutionary pathways reverting from colonial forms back to solitary (Fig. 7); in
387 addition, each budding mode and common cloacal cavity have never been lost after they
388 were acquired. This tendency can also be observed broadly within Tunicata, with some
389 species within the diazonid genus *Rhopalaea* being hypothesized to have undergone an
390 evolutionary loss of budding (Alié et al. 2021). Likewise, very few species in Bryozoa
391 have secondarily acquired solitary forms (Schwaha et al. 2020); no example of
392 reversion from coloniality to solitary in hemichordates (cf. Cannon et al. 2013) and
393 kamptozoans (cf. Fuchs et al. 2010). In contrast, reversal evolution from colonial to
394 solitary forms (and vice versa) is not uncommon in cnidarians (e.g., McFadden et al.

2021).

Acknowledgements

We would like to express our sincere gratitude for the significant contribution to our sample collections in each field, made by Shoichi Hamano and Hidenori Katsuragawa (Akkeshi Marine Station, Hokkaido University) at Akkeshi Bay; Hisanori Kohtsuka (Misaki Marine Biological Station, the University of Tokyo) at Misaki; Masashi Fukuoka, Naoto Jimi, Misato Sako, and Maki Shirae-Kurabayashi (Sugashima Marine Biological Laboratory, Nagoya University) around Sugashima Island; Takeo Sugimoto (South Wakayama Fishery Cooperative), Natsumi Hookabe (Japan Agency for Marine-Earth Science and Technology, JAMSTEC), Cati (Association for the Protection of the Sea and Marine Life, *Umimorinchu*), Ayumi Mizutani, Takashi Okada, and Naofumi Ueda (Dive KOOZA) in Kushimoto and Koza; Hiroshi Kuriyama (Miyako Island Fishery Cooperative), Hiroki Iranami (Irabu Island Fishery Cooperative), Hiroshi Yonamine (Ikema Island Fishery Cooperative), Yosuke Kamata, Manami Kimura, Junko Watanabe (Aquastar Miyakojima), Yuki Kita, Hiroki Matsushita, Shoki Shiraki, and Aoi Tsuyuki (Hokkaido University) around Irabu Island and Miyako Island; Bar Gabso, Lion Novak (Tel-Aviv University), Nahum Sela (Interuniversity Institute for Marine

Sciences), and a volunteer diver at Interuniversity Institute for Marine Sciences, Shlomi Levi, in Eilat, Israel. Without the invaluable assistance given to NH provided by Gil Koplovitz (Interuniversity Institute for Marine Sciences) and Gal Vered (Tel-Aviv University) during NH's lab works at Interuniversity Institute for Marine Sciences, the goals of this research would not have been realized. A precious photograph of *Polyandrocarpa zorittensis* given by Teruaki Nishikawa improve the figure in this study. Our sincere thanks are offered for the academic support provided by Analytical Center of Suntory Foundation for Life Sciences Bioorganic Research Institute, SUNBOR in conducting RNA-seq analysis. We would like to extend our heartful thanks to Kei Kitahata, whose technical insights were a cornerstone in the creation of the scripts that enabled smooth progress in our phylogenomic analyses. We are deeply grateful to all the individuals who generously contributed to NH through the academic crowdfunding platform "academist"; special thanks go to Shunji Furukuma, Naoki Hayashi, Miyuki Honda, Hitoki Horie, Sho Hosotani, Yoshiki Iwai, Nami Kenmotsu, Moe, Takehiro Nakamura, Ryoma Nishikawa, Yuichi Sasaki, Tatsuya Shimoyama, Makoto Taniguchi, Daiki Wakita, Takaaki Yonekura, and many others. NH was granted financial support from JST SPRING, with Grant Number JPMASP2119.

References

Aberer AJ, Kobert K, Stamatakis A (2014) ExaBayes: massively parallel Bayesian tree inference for the whole-genome era. Molecular Biology and Evolution 31(10): 2553–2556.

Akhmadieva AV, Shukalyuk AI, Aleksandrova YN, Isaeva VV (2007) Stem cells in asexual reproduction of the colonial ascidian *Botryllus tubaratus* (Tunicata: Ascidiacea). Russian Journal of Marine Biology 33: 181–186.

Alié A, Hiebert LS, Scelzo M, Tiozzo S. (2021) The eventful history of nonembryonic development in tunicates. Journal of Experimental Zoology. Part B, Molecular and Developmental Evolution 336: 250–266.

Alié A, Hiebert LS, Simion P, Scelzo M, Prünster MM, Lotito S, Delsuc F, Douzery EJP, Dantec C, Lemaire P, Darras S, Kawamura K, Brown FD, Tiozzo S (2018) Convergent acquisition of nonembryonic development in styelid ascidians. Molecular Biology and Evolution 35(7): 1728–1743.

Barbeitos MS, Romano SL, Lasker HR (2010). Repeated loss of coloniality and symbiosis in scleractinian corals. Proceedings of the National Academy of Sciences of the United States of America 107: 11877–11882.

Beklemishev WN (1969) Principles of Comparative Anatomy of Invertebrates. Vol. 1, Promorphology. Oliver and Boyd, Edinburgh, xxx + 490 pp.

Berrill NJ (1940) The development of a colonial organism: *Symplegma viride.* Biological Bulletin 79: 272–281.

Berrill NJ (1948) The gonads, larvae, and budding of the polystyelid ascidians *Stolonica* and *Distomus*. Journal of the Marine Biological Association of the United Kingdom 27: 633–650.

Blueweiss L, Fox H, Kudzma V, Nakashima D, Peters R, Sams S (1978) Relationships between body size and some life history parameters. Oecologia 37: 257–272.

Braun K, Stach T (2018) Morphology and evolution of the central nervous system in adult tunicates. Journal of Zoological Systematics and Evolutionary Research 57(2): 323–344.

Bray NL, Pimentel H, Melsted P, Pachter L (2016) Near-optimal probabilistic RNA-seq quantification. Nature Biotechnology 34: 525–527.

Brown FD, Keeling EL, Le AD, Swalla BJ (2009) Whole body regeneration in a colonial zscidian, *Botrylloides violaceus*. Journal of Experimental Zoology. Part B, Molecular and Developmental Evolution 312: 885–900.

Brown FD, Swalla BJ (2012) Evolution and development of budding by stem cells: Ascidian coloniality as a case study. Developmental Biology 369: 151–162.

Brunetti R, Mastrototaro F (2004) The non-indigenous stolidobranch ascidian Polyandrocarpa zorritensis in the Mediterranean: description, larval morphology and pattern of vascular budding. Zootaxa 528: 1–8.

Burighel P, Cloney RA (1997) Urochordata: Ascidiacea. Pp. 221–347. In: Harrison FW, Ruppert EE (Eds) Microscopic Anatomy of Invertebrates 5: Hemichordata, Chaetognatha and the Invertebrate Chordates. Wiley-Liss, New York.

Cannon JT, Swalla BJ, Halanych KM (2013) Hemichordate molecular phylogeny reveals a novel cold-water clade of harrimaniid acorn worms. The Biological Bulletin 255: 194–204.

Capella-Gutiérrez S, Silla-Martinez JM, Gabaldon T (2009) trimAl: a tool for automated alignment trimming in large-scale phylogenetic analyses. Bioinformatics 25:1972–1973.

Chernomor O, von Haeseler A, Minh BQ (2016) Terrace aware data structure for phylogenomic inference from supermatrices. Systematic Biology 65: 997–1008.

Connell JH (1961) The influence of interspecific competition and other factors on the distribution of the barnacle *Chthamalus stellatus*. Ecology 42(4) 710–723.

Davidson B, Jacobs MW, Swalla BJ (2004) The individual as a module: metazoan evolution and coloniality. Pp. 443–465. In: Schlosser G, Wagner G (Eds) Modularity in Development and Evolution. University of Chicago Press, Chicago.

Dayton PK (1971) Competition, disturbance, and community organization: the provision and subsequent utilization of space in a rocky intertidal community. Ecological Monographs 41(4): 351–389.

Emms DM, Kelly S (2015) OrthoFinder: solving fundamental biases in whole genome comparisons dramatically improves orthogroup inference accuracy. Genome Biology 16: 157.

Ewing B, Hillier L, Wendl MC, Green P (1998) Base-calling of automated sequencer traces using Phred. I. Accuracy assessment. Genome Research 8(3): 175–185.

Felsenstein J (1973) Maximum-likelihood estimation of evolutionary trees from continuous characters. American Journal of Human Genetics 25(5): 471.

Freckleton RP (2012) Fast likelihood calculations for comparative analyses. Methods in Ecology and Evolution 3(5): 940–947.

Fu L, Niu B, Zhu Z, Wu S, Li W (2012) CD-HIT: accelerated for clustering the next generation sequencing data. Bioinformatics 28: 3150–3152.

Fuchs J, Iseto T, Hirose M, Sundberg P, Obst M (2010) The first internal molecular phylogeny of the animal phylum Entoprocta (Kamptozoa). Molecular Phylogenetics and Evolution 56: 370–379.

Giard A (1872) Recherches sur les ascidies composées ou synascidies. Archives de Zoologie Expérimentale et Générale 1: 501–687.

Grabherr MG, Haas BJ, Yassour M, Levin JZ, Thompson DA, Amit I, Adiconis X, Fan L, Raychowdhury R, Zeng Q, Chen Z, Mauceli E, Hacohen N, Gnirke A, Rhind N, di Palma F, Birren BW, Nusbaum C, Lindblad-Toh K, Friedman N, Regev A (2011) Full-length transcriptome assembly from RNA-seq data without a reference genome. Nature Biotechnology 29(7): 644–652.

Grischenko AV, Taylor PD, Mawatari SF (2002) A new cheilostome bryozoan with gigantic zooids from the north-west Pacific. Zoological Science 19: 1279–1289.

Gutierrez S, Brown FD (2017) Vascular budding in *Symplegma brakenhielmi* and the evolution of coloniality in styelid ascidians. Developmental Biology 423(2): 152–169.

Hasegawa N, Kajihara H (2019) A redescription of *Syncarpa composita* (Ascidiacea, Stolidobranchia) with an inference of its phylogenetic position within Styelidae. ZooKeys 857: 1–15.

Hiebert LS, Simpson C, Tiozzo S (2021) Coloniality, clonality, and modularity in animals: the elephant in the room. Journal of Experimental Zoology. Part B, Molecular and Developmental Evolution 336: 198–211.

Hoang DT, Chernomor O, von Haeseler A, Minh BQ, Vinh LS (2018) UFBoot2: improving the ultrafast bootstrap approximation. Molecular Biology and Evolution 35: 518–522.

Hughes RN (2005) Lessons in modularity: the evolutionary ecology of colonial invertebrates. Scientia Marina 69(Suppl. 1): 169–179.

Jackson JBC (1977) Competition on marine hard strata: the adaptive significance of solitary and colonial strategies. The American Naturalist 111(980): 743–767.

Jackson JBC (1985) Distribution and ecology of clonal and aclonal benthic invertebrates. Pp. 297–355. In: Jackson JBC, Buss LW, and Cook RE (Eds) Population Biology and Evolution of Clonal Organisms. Yale University Press, New Haven.

Kalyaanamoorthy K, Minh BQ, Wong T.K.F., von Haeseler A., Jermiin L.S. (2017) ModelFinder: fast model selection for accurate phylogenetic estimates. Nature Methods 14: 587–589.

Katoh K, Standley DM (2013) MAFFT multiple sequence alignment software version 7: improvements in performance and usability. Molecular Biology and Evolution 30(4): 772–780.

Kawamura K, Sunanaga T (2010) Hemoblasts in colonial tunicates: Are they stem cells or tissue-restricted progenitor cells? Development Growth and Differentiation 52(1): 69–76.

Kawamura K, Watanabe H (1981) Studies of Japanese compound styelid ascidians. III. A new, possibly asexual *Polyandrocarpa* from Shimoda Bay. Publications of the Seto Marine Biological Laboratory 4–6: 425–436.

Kayal E, Bentlage B, Pankey MS, Ohdera AH, Medina M, Plachetzki DC, Collins AG, Ryan JF (2018) Phylogenomics provides a robust topology of the major cnidarian lineages and insights on the origins of key organismal traits. BMC Evolutionary Biology 18: 68.

Kocot MK (2016) On 20 years of Lophotrochozoa. Organisms Diversity and Evolution 16: 329–343.

Kott P (1985) The Australian Ascidiacea. Part 1: Phlebobranchia and Stolidobranchia. Memoirs of the Queensland Museum 23: 1–440.

Li W, Godzik A (2006) CD-HIT: a fast program for clustering and comparing large sets of protein or nucleotide sequence. Bioinformatics 22: 1658–1659.

Liow LS, Taylor PD (2019) Cope's rule in a member organism: Directional evolution without an overarching macroevolutionary trend. Evolution 73: 1863–1872.

Manni M, Berkeley MR, Seppey M, Simao FA, Zdobnov EM (2021) BUSCO update: novel and streamlined workflows along with broader and deeper phylogenetic coverage for scoring of eukaryotic, prokaryotic, and viral genomes. Molecular Biology and Evolution 38(10): 4647–4654.

McFadden CS, Quattrini AM, Brugler MR, Cowman PF, Dueñas LF, Kitahara MV, Paz-García DA, Reimer JD, Rodríguez E (2021) Phylogenomics, origin, and diversification of anthozoans (Phylum Cnidaria). Systematic Biology 70(4): 635–647.

Metschnikoff E (1869) Uber die Larven und Knospen von *Botryllus*. Bulletin de l'Académie Impériake des Sciences de Saint‐Pétersbourg 13: 293–298.

Minh BQ, Schmidt HA, Chernomor O, Schrempf D, Woodhams MD, von Haeseler A, Lanfear R (2020) IQ-TREE 2: New models and efficient methods for phylogenetic inference in the genomic era. Molecular Biology and Evolution 37(5): 1530–1534.

Monniot C, Monniot F, Laboute P (1991) Coral reef ascidians of New Caledonia. ORSTOM, Paris, 247 pp.

Mukai H (2001) Biology of colonial animals. Publication Committee for Biology of Colonial Animals, Tokyo, 117pp. [In Japasenese]

Mukai H, Watanabe, H (1976). Studies on the formation of germ cells in a compound ascidian *Botryllus primigenus* Oka. Journal of Morphology 148: 337–362.

Nakauchi M (1982) Asexual development of ascidians: its biological significance, diversity, and morphogenesis. American Zoologist 22: 753–763.

Nanglu K, Cole SR, Wright DF, Souto C (2023) Worms and gills, plates and spines: the evolutionary origins and incredible disparity of deuterostomes revealed by fossils, genes, and development. Biological Reviews 98: 316–351.

Oka H, Watanabe H (1957) Vascular budding, a new type of budding in *Botryllus*. The Biology Bulletin 112(2): 225–240.

Pagel M (1999) Inferring the historical patterns of biological evolution. Nature 401(6756): 877–884.

Pagel M, Meade A, Barker D (2004) Bayesian estimation of ancestral character states on phylogenies. Systematic Biology 53(5): 673–684.

Paine RT (1971) A short-term experimental investigation of resource partitioning in a New Zealand rocky intertidal habitat. Ecology 62: 1096–1106.

Pequegnat WE (1964) The epifauna of a California siltstone reef. Ecology 45: 272–283.

Pérez-Portela R, Bishop JDD, Davis AR, Turon X (2009) Phylogeny of the families Pyuridae and Styelidae (Stolidobranchiata, Ascidiacea) inferred from mitochondrial and nuclear DNA sequences. Molecular Phylogenetics and Evolution 50: 560–570.

Pizon A (1893) Histoire de la blastogénèse chez les *Botryllides*. Annales de Sciences Naturelles 7(14) 1–386.

Redikorzev V (1913) Neue Ascidien. Zoologischer Anzeiger 43: 204–213.

Ritter WE (1896) Budding in compound ascidians based on studies on *Goodsiria* and *Perophora*. Journal of Morphology 12: 149–238.

Ryland JS, Warner GF (1986) Growth and form in modular animals: ideas on the size and arrangement of zooids. Philosophical Transactions of the Royal Society of London B 313: 53–76.

Sabbadin A., Zaniolo G, Majone F (1975) Determination of polarity and bilateral asymmetry in palleal and vascular buds of the ascidian *Botryllus schlosseri*. Developmental Biology 46(1): 79–87.

Sanamyan K (2000) Ascidians from the north-western Pacific region 7. Styelidae. Ophelia 53(1): 67–78.

Satoh N (1994) Developmental Biology of Ascidians. Cambridge University Press, New York, 251 pp.

Schwaha TF, Ostrovsky AN, Wanninger A (2020) Key novelties in the evolution of the aquatic colonial phylum Bryozoa: evidence from soft body morphology. Biological Reviews 95: 696–729.

Selys-Longchamps MD (1917) Sur le bourgeonnement des Polystiélinés *Stolonica* et *Heterocarpa* avec quelques notes sur l'anatomie de ces deux genres. Bulletin Scientifique de la France et de la Belgique 3: 170–276.

Seppey M, Manni M, Zdobnov EM (2019) BUSCO: assessing genome assembly and annotation completeness. Pp. 227–245. In: Kollmar M (Ed) Gene Prediction. Methods in Molecular Biology, vol 1962. Humana, New York.

Shirae M, Hirose E, Saito Y (1999) Behavior of hemocytes in the allorejection reaction in two compound ascidians, *Botryllus scalaris* and *Symplegma reptans*. Biology Bulletin 197: 188–197.

Simão FA, Waterhouse RM, Ioannidis P, Kriventseva EV, Zdobnov EM (2015) BUSCO: assessing genome assembly and annotation completeness with single-copy orthologs. Bioinformatics 31(19): 3210–3212.

Simion P, Belkhir K, François C, Veyssier J, Rink JC, Manuel M, Philippe H, Telford MJ (2018) A software tool 'CroCo' detects pervasive cross-species contamination in next generation sequencing data. BMC Biology 16: 28.

Sogot CE, Harper EM, Taylor PD (2014) The lilliput effect in colonial organisms: cheilostome bryozoans at the Cretaceous–Paleogene mass extinction. PLOS ONE 9(2): e87048.

Tokioka T (1951) The fauna of Akkeshi Bay XVIII. Ascidia. Publications from the Akkeshi Marine Biological Station 1: 1–22, 2 pls.

Tsagkogeorga G, Turon X, Hopcroft RR, Tilak M, Feldstein T, Shenkar N, Loya Y, Huchon D, Douzery EJP, Delsuc F (2009) An updated 18S rRNA phylogeny of tunicates based on mixture and secondary structure models. BMC Evolutionary Biology 9: 187.

Tyrrell MC, Byers JE (2007) Do artificial substrates favor nonindigenous fouling species over native species? Journal of Experimental Marine Biology and Ecology 342: 54–60.

Watanabe H, Tokioka T (1972) Two new species and one possibly new race of social styelids from Sagami Bay with remarks on their life history especially the mode of budding. Publications of the Seto Marine Biological Laboratory 195: 327–345.

Waterhouse RM, Seppey M, Simão FA, Manni M, Ioannidis P, Klioutchnikov G, Kriventseva EV, Zdobnov EM (2017) BUSCO applications from quality assessments to gene prediction and phylogenomics. Molecular Biology and Evolution 35(3): 543–548.

Zeng L, Jacobs MW, Swalla BJ (2006) Coloniality has evolved once in stolidobranch ascidians. Integrative and Comparative Biology 46(3): 255–268.

Figures and Tables

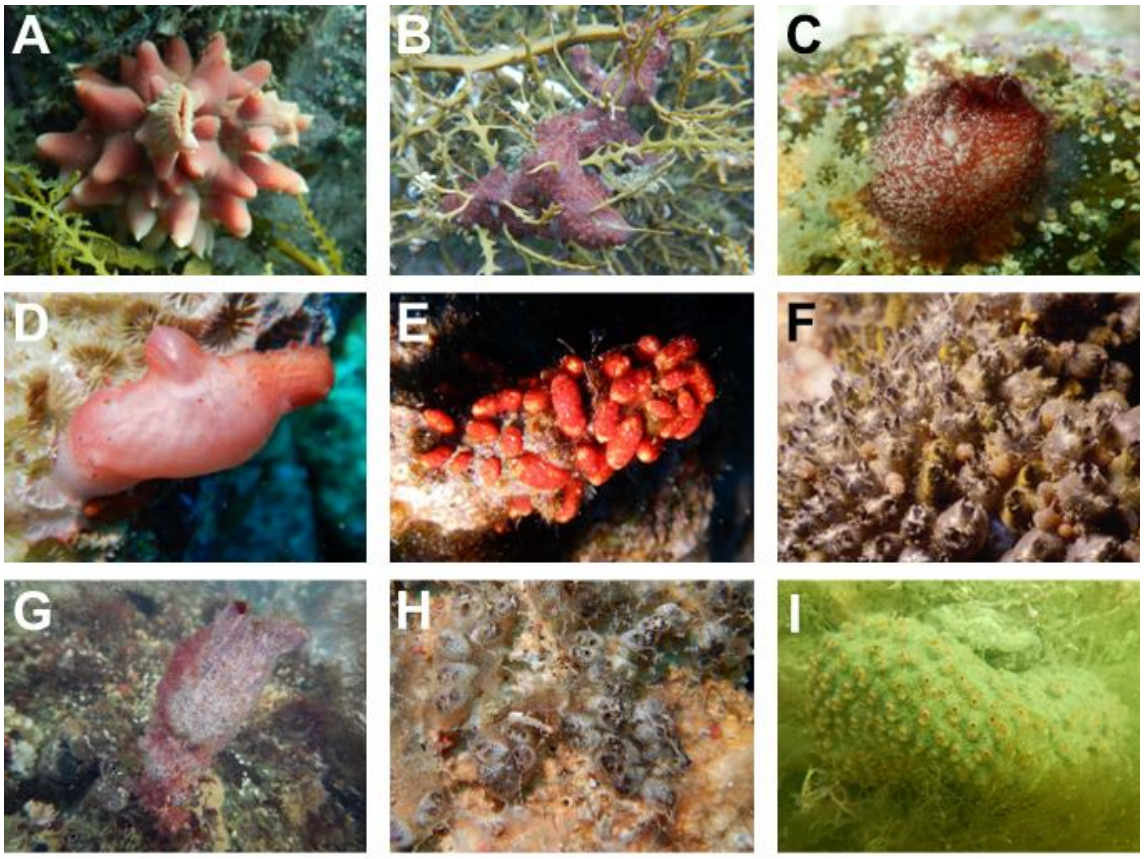

Figure 1. Solitary and colonial ascidians in Stolidobranchia. A, *Halocynthia roretzi*; B, *Botrylloides violaceus*; C, *Cnemidocarpa clara*; D, *Cnemidocarpa margaritifera*; E, *Eusynstyela latericius*; F, *Polyandrocarpa zorritensis* (photographed by Dr. Nishikawa); G, *Styela clava*; H; *Symplegma systematica*; I, *Syncarpa composita*.

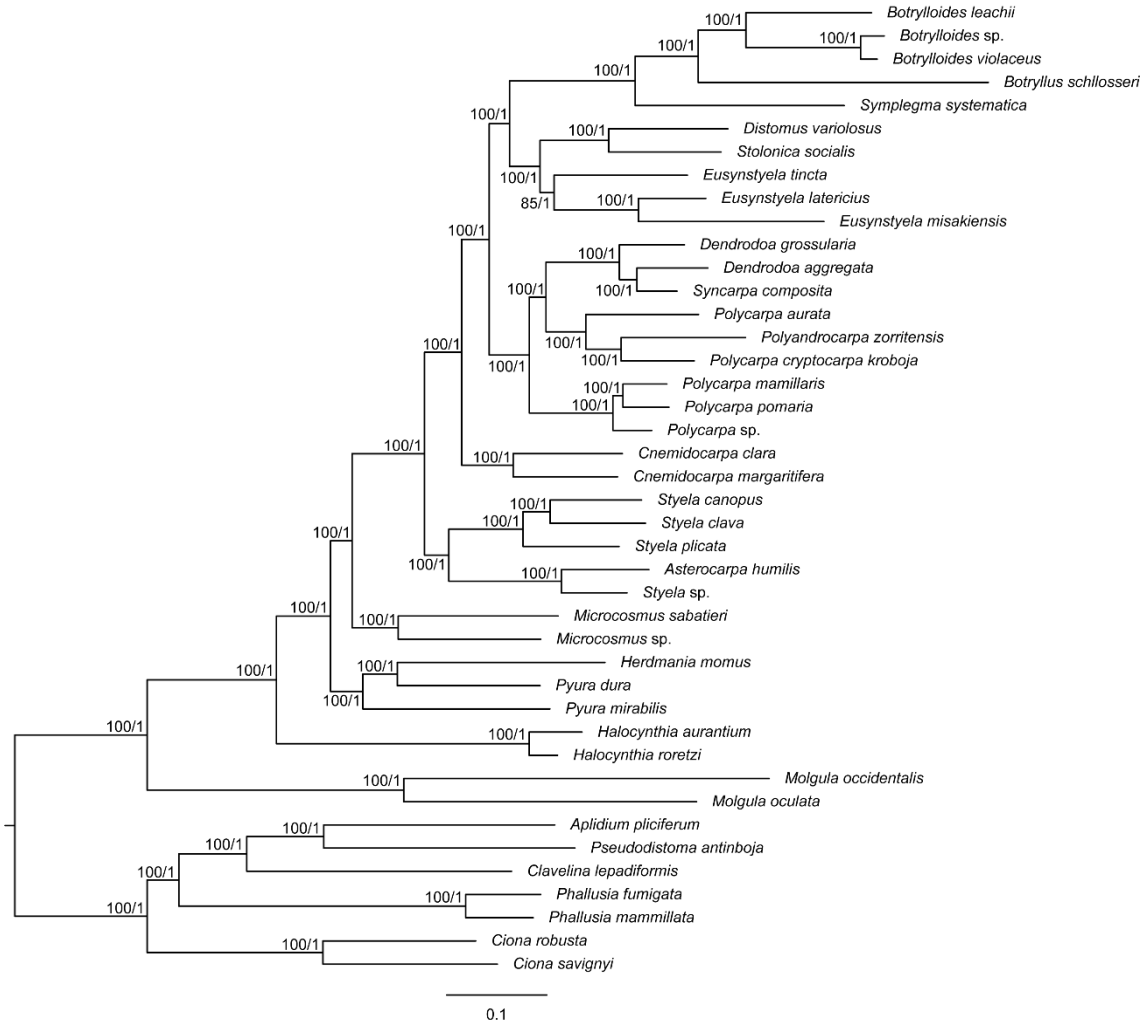

Figure 2. Maximum-likelihood tree based on 1,883 genes; the number on each branch indicates UF bootstrap value and PP.

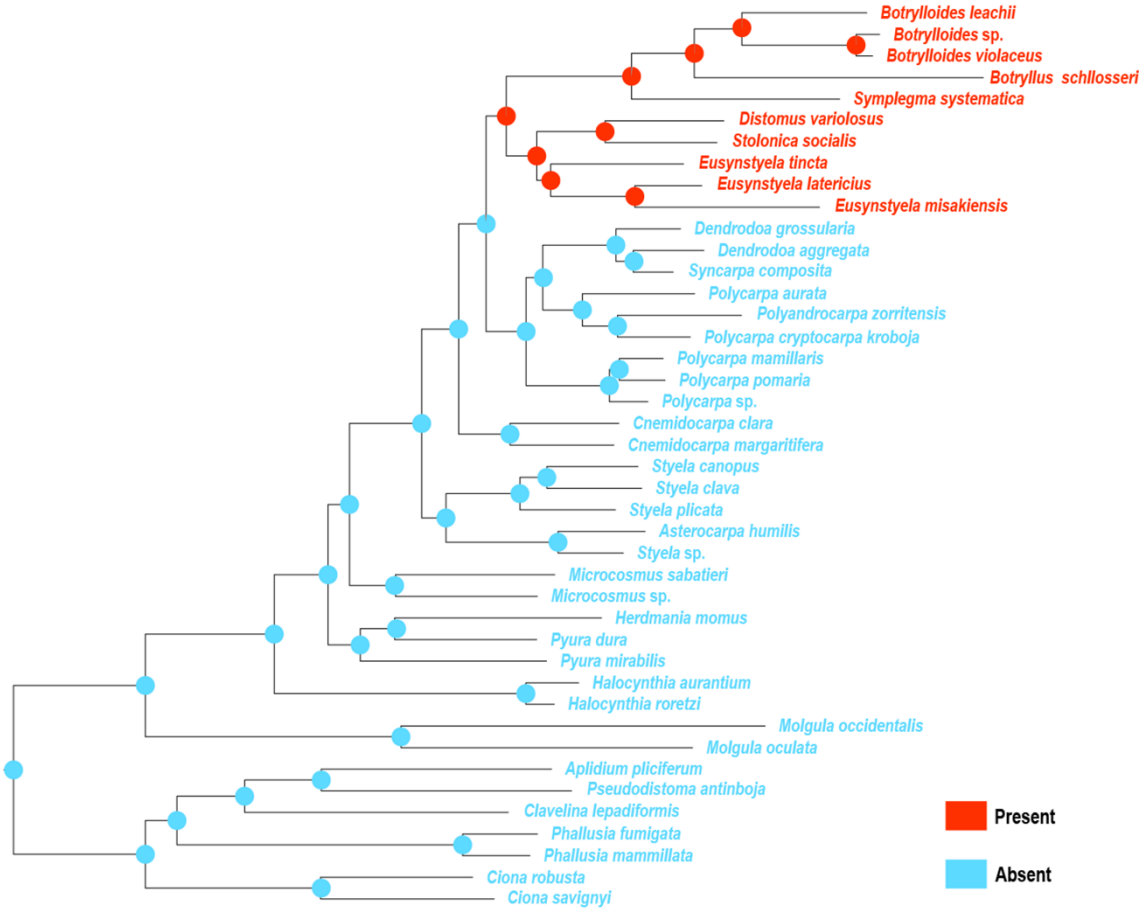

Figure 3. ML tree showing the presence of peribranchial budding. The pie charts indicate EAPs of the characteristics in the nodes.

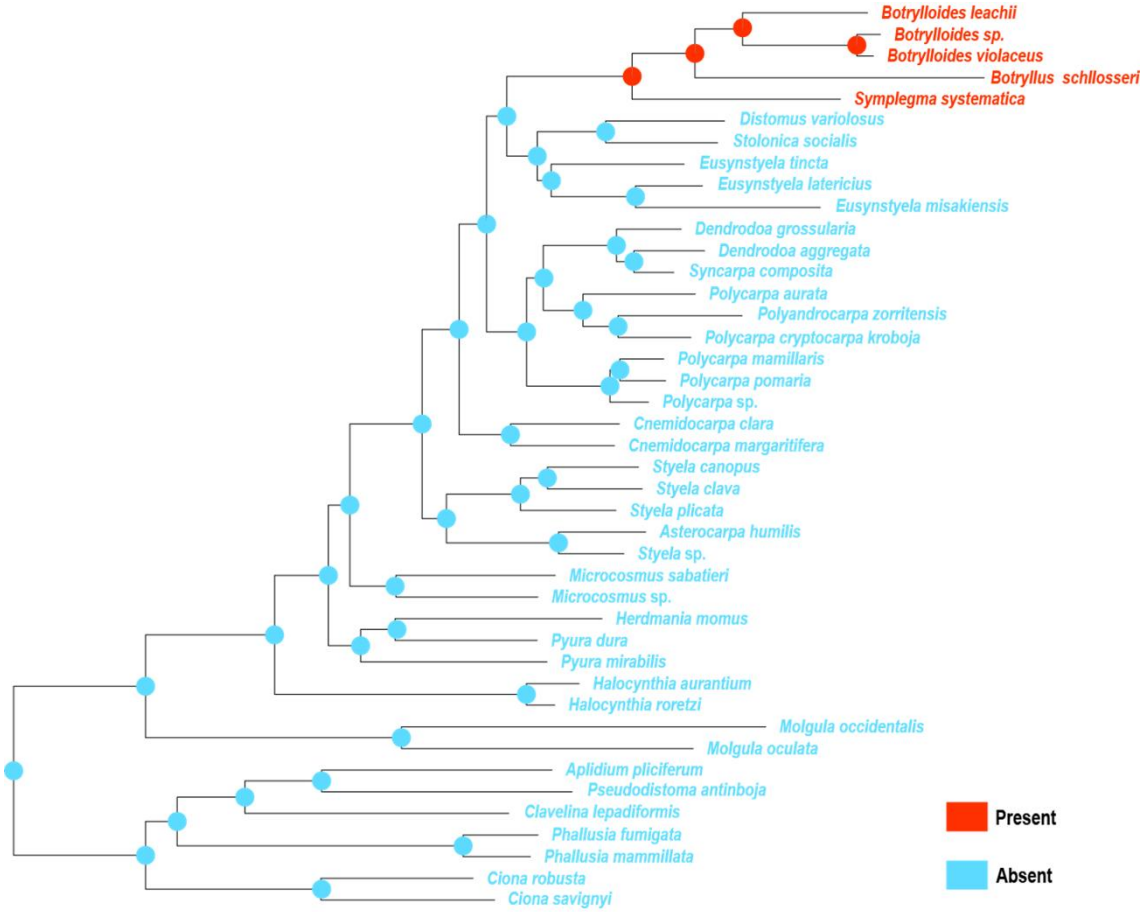

Figure 4. ML tree showing the presence of vascular budding. The pie charts indicate EAPs of the characteristics in the nodes.

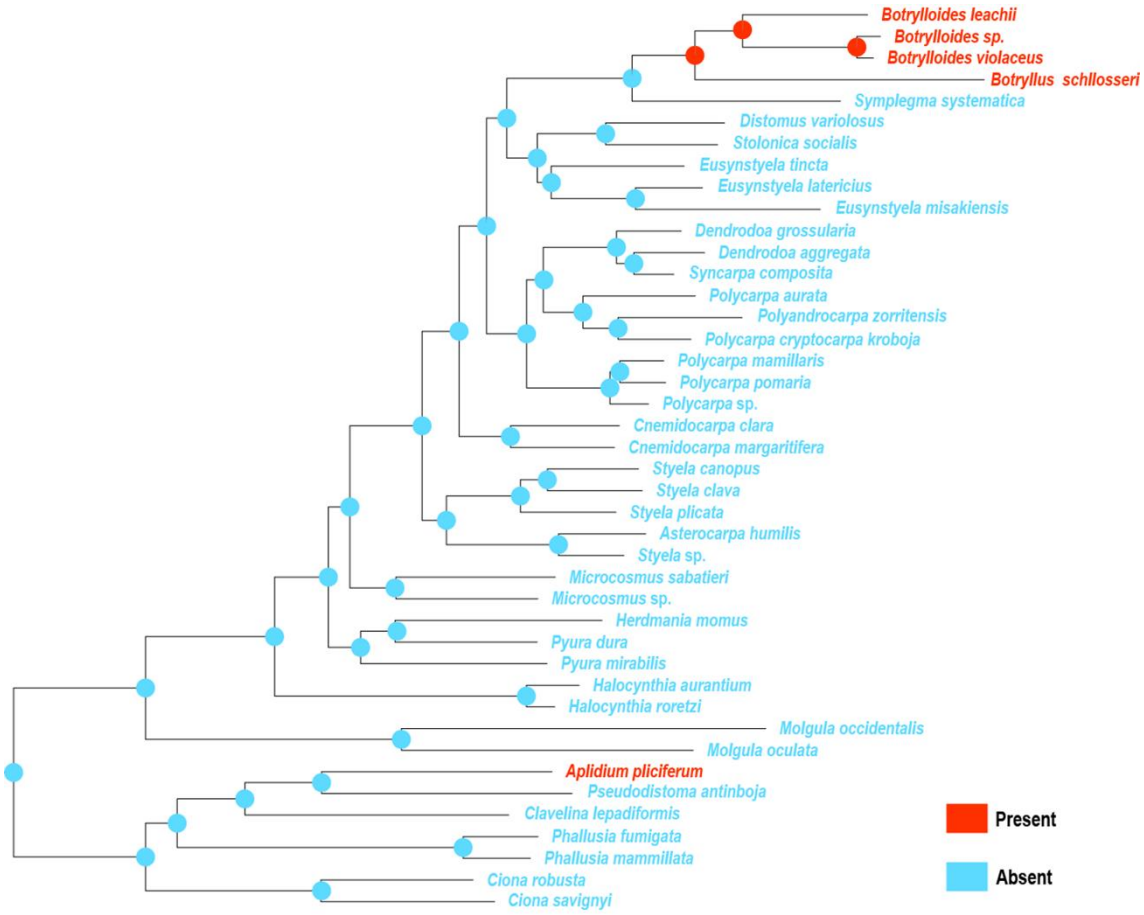

Figure 5. ML tree showing the presence of common cloacal cavity. The pie charts indicate EAPs of the characteristics in the nodes.

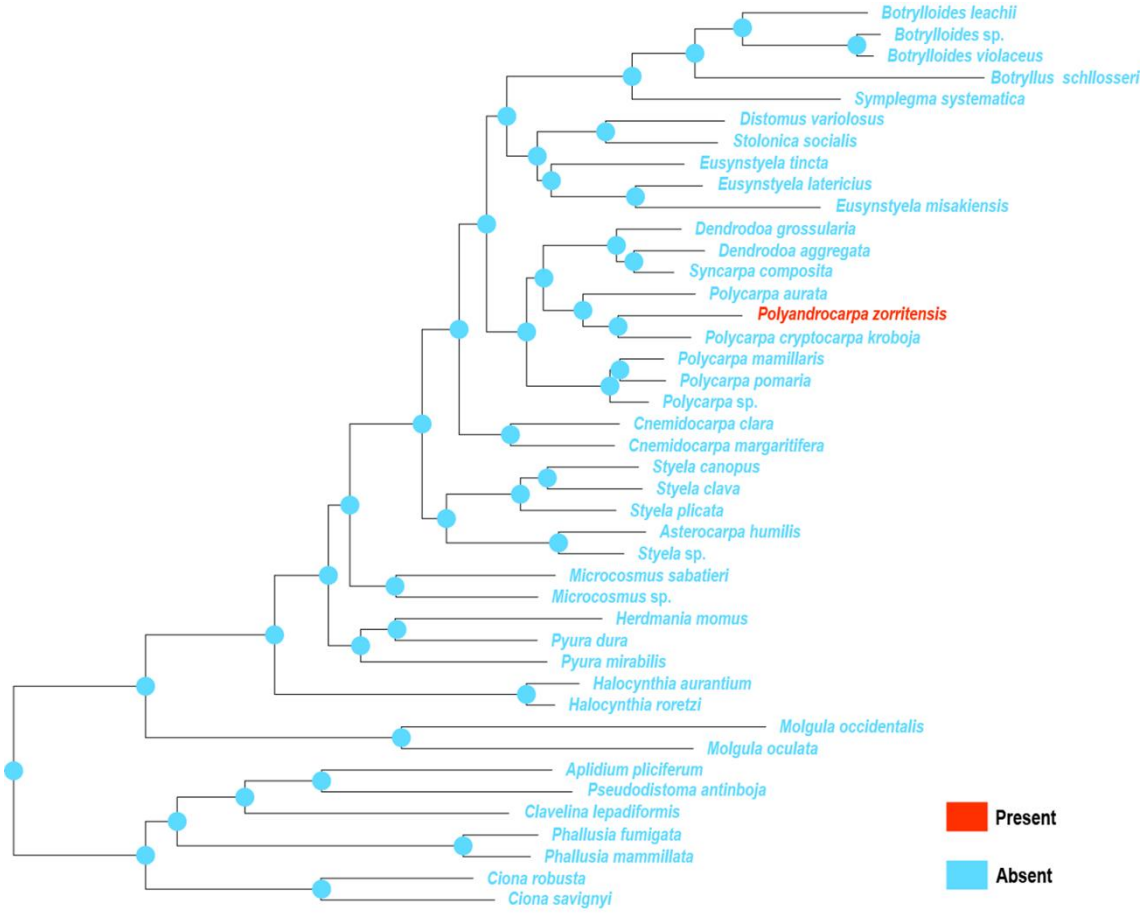

Figure 6. ML tree showing the presence of basal budding. The pie charts indicate EAPs of the characteristics in the nodes.

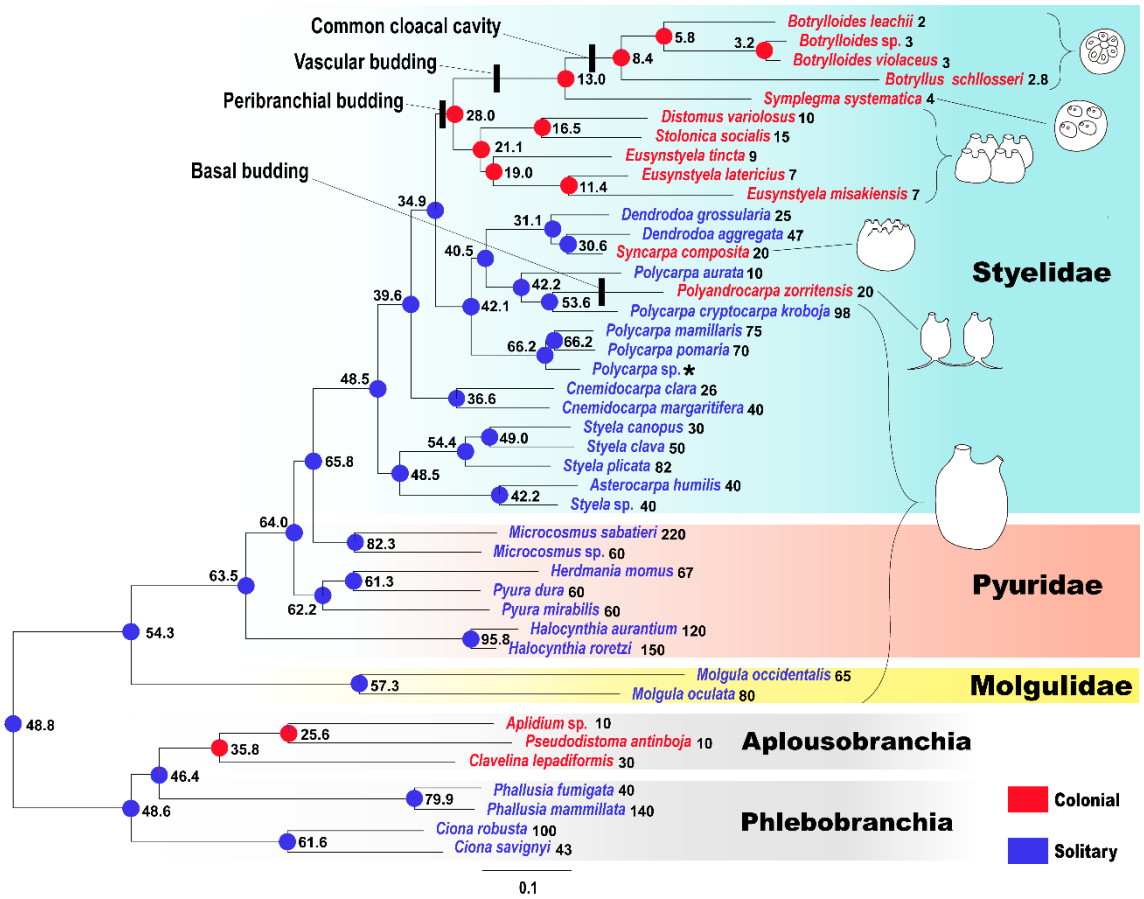

Figure 7. Evolutionary changes of coloniality and body length inferred by ancestral state reconstruction. Pie charts indicate EAPs that an ancestor at each node was colonial/solitary. The numbers show body length of ancestors and OTU; the body length of *Polycarpa* sp. was unknown, so it was indicated by asterisk (*).

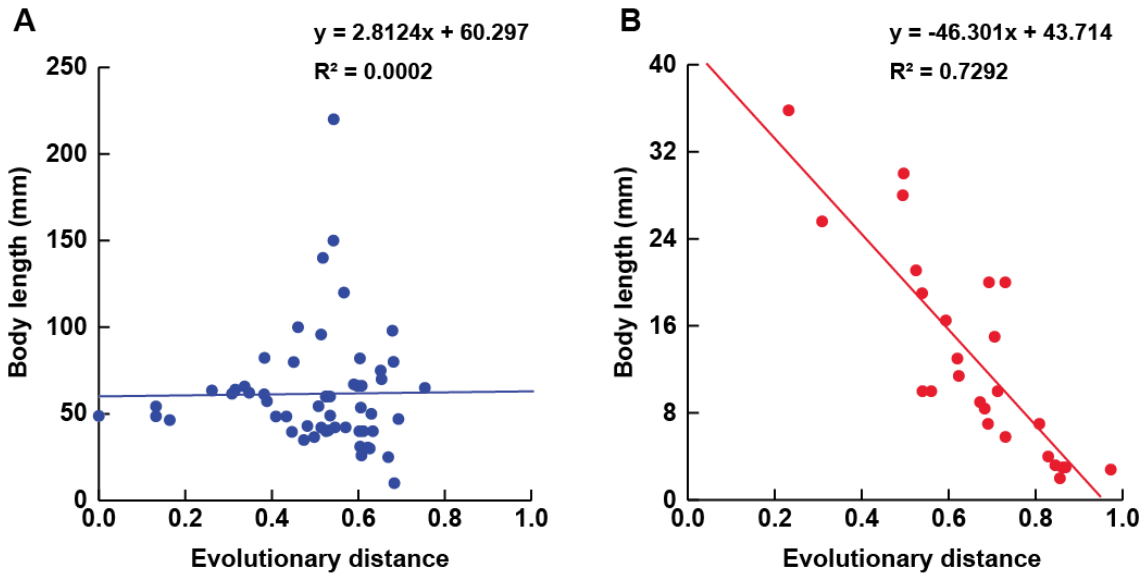

Figure 8. Relationship between body length and evolutionary distance in the OTUs and the nodes of the phylogenomic tree. A, solitary forms (n = 56); B, colonial forms (n = 25).

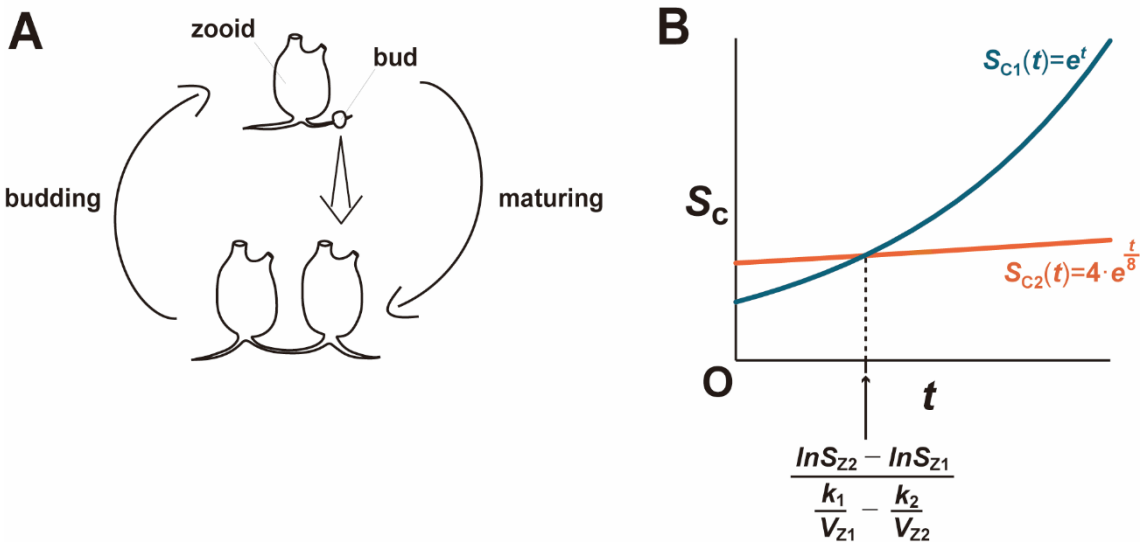

Figure 9. Illustrations of the relationship between zooid size and growth rate of a colony. A, asexual cycle of a budding colony; B, a graph representing two different colonies having similar geometrical structure (S_Z = 2 or 4; V_Z = 1 or 8; k = 1).

Table 1. Sample information including order, family, species name, sampling date, and sampling site.

Order	Family	Species	Sampling date	Sampling site
Aplousobranchia	Clavelinidae	*Clavelina lepadiformis* (Müller, 1776)	2021/5/12	Kushimoto, Japan
	Polyclinidae	*Aplidium* sp.	2022/3/9	Misaki, Japan
	Pseudodistomidae	*Pseudodistoma antinboja* Tokioka, 1949	2021/5/11	Koza, Japan
Stolidobranchia	Pyuridae	*Herdmania momus* (Savignyi, 1816)	2021/5/11	Koza, Japan
		Microcosmus sp.	2021/5/11	Koza, Japan
		Pyura mirabilis (Heller, 1877)	2021/11/1	Sugashima Island, Japan
	Styelidae	*Botrylloides* sp.	2022/3/15	Misaki, Japan
		Botrylloides violaceus Oka, 1927	2021/11/1	Sugashima Island, Japan
		Cnemidocarpa clara (Hartmeyer, 1906)	2021/11/1	Sugashima Island, Japan
		Cnemidocarpa margaritifera Michaelsen, 1918	2023/1/18	Eilat, Israel
		Eusynstyela latericius (Sluiter, 1904)	2023/1/16	Eilat, Israel
		Eusynstyela misakiensi (Watanabe and Tokioka, 1972)	2021/5/11	Koza, Japan
		Polycarpa cryptocarpa kroboja (Sluiter, 1885)	2021/11/1	Sugashima Island, Japan
		Dendrodoa aggregate (Rathke, 1806)	2022/6/10	Akkeshi, Japan
		Styela sp.	2022/3/15	Misaki, Japan
		Symplegma systematica (Sluiter, 1904)	2022/4/23	Irabujima Island, Japan
		Syncarpa composita (Tokioka, 1951)	2022/6/30	Akkeshi, Japan

Table 2. Sequence data obtained from the GitHub repository styelidae and ANISEED.

Order	Family	Species	Source
Phlebobranchia	Ascidiidae	*Phallusia fumigata* (Grube, 1864)	ANISEED
		Phallusia mammillata (Cuvier, 1815)	ANISEED
	Cionidae	*Ciona robusta* Hoshino and Tokioka, 1967	ANISEED
		Ciona savignyi Herdman, 1882	ANISEED
Stolidobranchia	Molgulidae	*Molgula occidentalis* Traustedt, 1883	ANISEED
		Molgula oculata Forbes, 1848	ANISEED
	Pyuridae	*Halocynthia aurantium* (Pallas, 1787)	ANISEED
		Halocynthia roretzi (Drasche, 1884)	ANISEED
		Microcosmus sabatieri Roule, 1885	styelidae
	Styelidae	*Asterocarpa humilis* (Heller, 1878)	styelidae
		Botryllus schlosseri (Pallas, 1766)	ANISEED
		Botrylloides leachii (Savigny, 1816)	styelidae
		Dendroda grossularia (Van Beneden, 1846)	styelidae
		Distomus variolosus Gaertner, 1774	styelidae
		Eusynstyela tincta (Van Name, 1902)	styelidae
		Polyandrocarpa zorritensis (Van Name, 1931)	styelidae
		Polycarpa aurata (Quoy and Gaimard, 1834)	styelidae
		Polycarpa mamillaris (Pallas, 1774)	styelidae
		Polycarpa sp.	styelidae
		Stolonica socialis Hartmeyer, 1903	styelidae
		Styela canopus (Savigny, 1816)	styelidae
		Styela clava Herdman, 1881	styelidae
		Styela plicata (Lesueur, 1823)	styelidae

696 **Table 3.** The longest body length and coloniality of each species.

Order	Family	Species	Coloniality	Length (mm)	source of length
Aplousobranchia	Clavelinidae	*Clavelina lepadiformis*	colonial	30	this study
	Polyclinidae	*Aplidium pliciferum*	colonial	20	this study
	Pseudodistomidae	*Pseudodistoma antinboja*	colonial	10	this study
Phlebobranchia	Ascidiidae	*Phallusia fumigata*	solitary	40	Julin and Robert (1913)
		Phallusia mammillata	solitary	140	Millar (1970)
	Cionidae	*Ciona robusta*	solitary	100	Hoshino and Tokioka (1967)
		Ciona savignyi	solitary	43	Nishikawa (1991)
Stolidobranchia	Molgulidae	*Molgula occidentalis*	solitary	65	Van Name (1945)
		Molgula oculata	solitary	80	Monniot (1969)
	Pyuridae	*Halocynthia aurantium*	solitary	120	Nishikawa (1991)
		Halocynthia roretzi	solitary	150	Nishikawa (1991)
		Herdmania momus	solitary	67	Nishikawa (1991, 2002)
		Microcosmus sabatieri	solitary	220	Monniot (1962)
		Microcosmus sp.	solitary	60	this study
		Pyura dura	solitary	60	Heller (1877)
		Pyura mirabilis	solitary	60	Nishikawa (1991)
	Styelidae	*Asterocarpa humilis*	solitary	40	Kott (1985)
		Botrylloides leachii	colonial	2	Kott (1985)
		Botrylloides violaceus	colonial	3	Saito and Okuyama (2003)
		Botrylloides sp.	colonial	3	this study
		Botryllus schllosseri	colonial	2.8	Saito and Okuyama (2003)

Cnemidocarpa clara	solitary	26	Nishikawa (1991)
Cnemidocarpa margaritifera	solitary	40	Monniot (1973)
Dendrodoa aggregata	solitary	47	Nishikawa (1991)
Dendrodoa grossularia	solitary	25	Berrill (1950)
Distomus variolosus	colonial	10	Millar (1970)
Eusynstyela latericius	colonial	7	Tokioka (1967), Kott (1985)
Eusynstyela misakiensis	colonial	7	Watanabe and Tokioka (1972)
Eusynstyela tincta	colonial	9	Van Name (1945)
Polyandrocarpa zorritensis	colonial	20	Van Name (1945)
Polycarpa aurata	solitary	10	Kott (1985)
Polycarpa cryptocarpa kroboja	solitary	98	Nishikawa (1991)
Polycarpa mamillaris	solitary	75	Vazques et al. (1995)
Polycarpa pomaria	solitary	70	Brunetti and Mastrototaro (2017)
Polycarpa sp.	solitary	—	—
Stolonica socialis	colonial	15	Berrill (1948)
Styela canopus	solitary	30	Nishikawa (1995)
Styela clava	solitary	50	Nishikawa (1991)
Styela plicata	solitary	82	Nishikawa (1991)
Styela sp.	solitary	40	this study
Symplegma systematica	colonail	4	Nishikawa (1984)
Syncarpa composita	colonail	20	Hasegawa and Kajihara (2019)

699 **Table 4.** Number of reads and contigs of each species among each step of quality control.

Species	Number of reads	Trinity	Transdecoder	CD-HIT	min TPM	CroCo	ratio	Busco Index (%)
Clavelina lepadiformis	56682322	126660	122351	36843	36843	36843	29.1	96.3
Aplidium pliciferum	55774938	115622	95490	39219	39219	39219	33.9	94.1
Pseudodistoma antinboja	61465810	253926	130804	50694	50694	50694	20.0	94.9
Herdmania momus	42434406	88008	89631	26116	26116	26116	29.7	94
Microcosmus sp.	54163154	87164	106927	30896	30896	30896	35.4	95.6
Pyura mirabilis	43199584	83141	89898	29224	29224	29224	35.1	92.5
Botrylloides sp.	137362636	201787	137979	65432	65432	65432	32.4	96
Botrylloides violaceus	122384370	147738	112922	49286	49286	49286	33.4	95.8
Cnemidocarpa clara	43854848	114765	96283	34223	34223	34223	29.8	93.4
Cnemidocarpa margaritifera	44546458	72124	89219	27893	27893	27893	38.7	94.4
Eusynstyela latericius	124303040	344331	146190	74497	74497	74497	21.6	92.8
Eusynstyela misakiensi	127341340	327188	265280	108633	108633	108633	33.2	99.2
Polycarpa cryptocarpa kroboja	51953554	130749	122330	46481	46481	46481	35.5	95.3

Dendrodoa aggregata	46787562	172013	157965	71393	71393	71393	41.5	97.4
Styela sp.	56036346	140726	120963	43202	43202	43202	30.7	96.5
Symplegma systematica	126899150	314471	126874	64540	64540	64540	20.5	93.4
Syncarpa composita	134010390	501552	229526	99555	99555	99555	19.8	94.4

702